# CROSS AND CLOVER SHAPED ORIFICE JETS ANALYSIS AT LOW REYNOLDS NUMBER

by

***Amina MESLEM*** [a*] ***and Ilinca NASTASE*** [b]

[a] Laboratory of Environmental Engineering, Center of Science and Technologie, University of La Rochelle, La Rochelle, France
[b] CAMBI, Technical University of Civil Engineering in Bucharest, Building Services Department, Bucharest, Romania

Original scientific paper
DOI: 10.2298/TSCI130724166M

*The jet coming from a cross-shaped orifice with an open center has been shown in the past, to provide substantial increase in the near field convective transport-mixing, in comparison to a classical round orifice jet.*
*Detailed information has been reported in previous works on the role played in the jet mixing enhancement by the crow of vortices composed of counter-rotating pairs of secondary streamwise structures which are developing in orifice's troughs. A trough in the cross-shaped jet generates a local shear like the one generated by a triangular tab in a square jet. In the present study we are interested by the modification of local shears in the troughs of the cross-shaped jet, when orifice geometry is modified, such as the center of the orifice becomes closed, leading to a clover-shaped orifice. The general motivation is to understand the effect of using a set of combination of longitudinal structures, themselves produced by the superposition of local shear regions, in mixing performance of a cross jet. It is shown that lower entrainment rates in the clover jet is a results of an additional internal crown of vortices which opposes the external one due to inner shears generated by closing the center of the orifice.*

Key words: *clover jet, cross jet, switching-over, entrainment, jet throw*

## Introduction

In the 20$^{th}$ century there were significant developments in research on free jet flows and it was initially believed that the statistically describable behaviour of a jet flow is totally independent of the conditions near the nozzle. The discovery of large structures of the jet [1-6] in the mixing layer and in the developing region (within the first few diameters of the nozzle) started a new trend of investigations: (1) attempting to assess the connection between the characteristics of the large scale structures and mass/momentum transport and/or flow behaviour, [2, 7-11] among others, and (2) attempting to control the dynamics of these structures and their effects on transport mechanisms in the flow, [12-19] among others. The jet control can be achieved by active or passive procedures. Such a control of jet flows have been widely used in applications such as to improve combustion efficiency, to reduce pollutants in mixing cham-

* Corresponding author; e-mail: ameslem@univ-lr.fr, amina.meslem@univ-rennes1.ft

bers and to attenuate ejectors noise in aircraft. Passive control could be preferred to the active one as it uses no external energy to control the jet dynamics. Passive control using lobed jets is based on geometrical manipulation of diffuser nozzles [16, 19, 20]. The underlying concept is to stretch the mixing layer in contact with the ambience in order to increase entrainment and spreading. Nozzle manipulation causes considerable modification of the large-scale vortices in their number, their shape and interaction, leading to considerable changes in jet mixing performance [16, 19, 20].

The role played by the Kelvin-Helmholtz (K-H) azimuthal rings and the streamwise vortices in the entrainment process in the near field of a round free orifice jet have been qualitatively and quantitatively analysed in our previous investigations, for a Reynolds number of 800 [21, 22] and 3600 [20], respectively. A strong correlation between the entrainment rate and the K-H vortex dynamics was found for both flow regimes. The K-H ring controls the sign of the radial velocity and the entrainment is mainly produced in the upstream part of the K-H ring as well as in the braid region where the streamwise vortices appear. In the downstream part of the K-H ring, the flow expands from the jet core to the surrounding. Hence, the K-H ring passing generates periodical compression/depression cycles in the round jet, which are believed to contribute to ambient air engulfment towards the jet core, but at the same time opposes the induction when the ring is approaching at a given axial position (*i. e.* in the downstream part of the ring). In our previous studies the dynamics of the round jet have been considered as a reference in the investigation of lobed jets (cross-shaped and daisy-shaped) having the same exit diameter and initial volume flow rate. It was found that large streamwise structures generated by the lip of the lobed diffuser are present. For the lobed jet, entrainment and expansion coexist in a practically unchanged manner in the presence or not of a K-H structure. The lobed orifice geometry introduces a transverse shear in the lobe troughs, like the one generated by a triangular tabs in a square jet [23], conducting to a breakdown of the K-H structures into *ring segments*. Streamwise structures continuously develop in the lobe troughs, at the resulting discontinuity regions, and control the ambient air entrainment. In this case the entrainment rate is less affected by the dynamics of the K-H structure and achieves higher levels that in the reference round jet.

In the present study we are trying to analyze what influence the lobe shape of the cross-shaped orifice plays in the shear produced by the lobes, in the resulting vortical mechanisms, and in the corresponding mixing performance. We focus on the particular case where the center of the cross-shaped orifice becomes closed leading to a clover-shaped orifice. This modification can be considered as an adjunction of a bluff body in the center of a nozzle, which is often used as flame holder in combustors, to enhance the blow-off limit and flame stability [24]. Our motivation is to understand the effect of using inner shear regions in entrainment capability of a cross-shaped jet. Although the two lobed jets considered in this study are cross-shaped, in the following, *cross-shaped orifice* will be reserved to the one with and an open center, whereas, the cross orifice having a closed center, is named *clover-shaped orifice*.

## Experimental procedures

Two isothermal air lobed jets are generated from a cross-shaped and a clover-shaped orifices having the same equivalent diameter $D_e = 10$ mm based upon the exit area $S$, $D_e = (4S/\pi)^{1/2}$, (fig. 1). The lobed jets are compared to a reference jet issued from a round orifice of 10 mm in diameter $D$. The orifices are built-up from aluminum sheet with 1.5 mm in thickness. The air jet experimental facility, fig. 1(b), consists of an axial miniature fan placed inside a metallic pipe having 1.00 m in length and 0.16 m in diameter. A convergent and a honeycomb were placed at the end of the pipe in order to reduce the turbulence level at the nozzle exit.

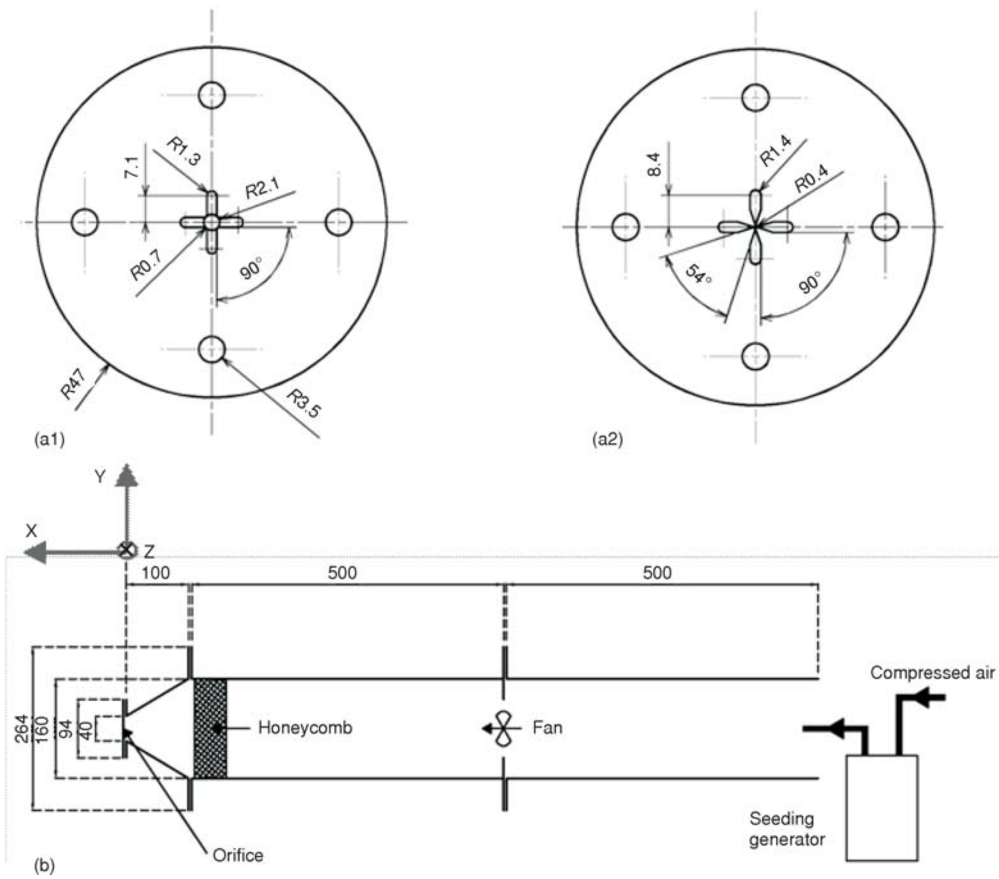


**Figure 1. (a) Orifices geometry: (a1) cross-shaped orifice, (a2) clover-shaped orifice; (b) experiment set-up**

Mean velocity fields measurements employed a 2-D Dantec laser doppler anemometer (LDA) system. The LDA system is compact and has two solid lasers: one ND:YAG of 25 mW (532 nm) and one Sapphire of 22 mW (488 nm). The sampling time during measurements was in the range of 60 to 100 s and the mean data rate ranged between 0.5 to 5 kHz depending on the flow velocity at the measurement point. The measuring volume at the lasers beam intersection is $0.04 \times 0.045 \times 0.378$ mm large. The probe was mounted on a 3-D traverse system with the ranges on the X-, Y-, and Z-axis, of 690 mm, 2020 mm, and 690 mm, respectively, and the movement resolution and reproducibility of 6.25 μm. The data were acquired on a grid in the (YZ) plane at each X location. The grid spacing varied from 0.25 mm to 2 mm with the streamwise distance X. The air jet flows were seeded with small paraffin oil droplets, 3 through 5 μm in diameter, provided by a liquid seeding generator from Dantec.

The uncertainty of the LDA measurement was estimated to be in the range of ±0.1 to ±0.6% for the $U$ and $V$ mean components, and in the range of ±1 to ±5% for the corresponding root mean square (RMS) velocities. This estimation is based on the evaluation of a global bias error, depending on all the parameters susceptible to bias the measurements and of a statistical uncertainty related to the data scattering around the mean values.

Transverse mean velocity fields from LDA measurements, are used to compute the 2-D velocity gradient tensor $\nabla u$ of the in-plane components ($V$, $W$), and to deduce the out-of-plane vorticity component, in its normalized form $\omega_X = [(\partial V/\partial Z) - (\partial W/\partial Y)(D_e/U_{0max})]$, and the $\lambda_2$ criterion proposed by [25].

The $\lambda_2$ criterion is a method employing velocity gradient tensor $\nabla u$. The velocity gradient tensor of a 3-D velocity field can be decomposed into its symmetric and anti-symmetric components, $\nabla u = S + \Omega = 1/2(\nabla u + \nabla u') + (1/2)(\nabla u - \nabla u')$, *i. e.*, into the tensors of rate-of-strain and of vorticity, respectively. By intuition, the vector of the local vorticity $\omega = \nabla \times u$, may serve as an indicator for the existence and strength of a vortical structure. However, the extraction of vortices and evaluation of their characteristics based purely on the vorticity modulus may fail in boundary layers and free shear layers [25, 26]. For instance, vortical structures present in shear layers tend to be obscured by vorticity without any swirling motion that is of the same order of magnitude as the shear strain rate.

The $\lambda_2$ criterion requires the second largest eigenvalue $\lambda_2$ of the symmetric tensor $S^2 + \Omega^2$ to be negative. The symmetric part of the gradient of the incompressible Navier-Stokes equations, neglecting unsteady and viscous effects, $S^2 + \Omega^2 = (-1/\rho)\nabla(\nabla p)$, can be used to identify swirling flow regions with a local pressure minimum. This requires two of three (real) eigenvalues of the (symmetric) pressure tensor to be negative. Hence, two eigenvalues of $S^2 + \Omega^2$ (where $\lambda_1 \geq \lambda_2 \geq \lambda_3$ have to be negative, and in particular $\lambda_2(S^2 + \Omega^2) < 0$. The second invariant of $\nabla u$ is related to the eigenvalues of $S^2 + \Omega^2$ as, $Q = (-1/2)tr(S^2 + \Omega^2) = (-1/2)(\lambda_1 + \lambda_2 + \lambda_3)$ [25].

## Jet initial conditions

The inlet flow rate for the two lobed jets and the reference round jet is $7.57 \cdot 10^{-5}$ ±3%. The initial exit Reynolds number based on the maximum exit velocity ($U_{0max}$) and the equivalent diameter is equal to 813 (tab. 1).

**Table 1. Jet inlet conditions**

| Orifice | $U_{0C}$ | $U_{0max}$ | $Re_0$ | $\theta_0$ [mm] | | $f_n$ [Hz] | $St_\theta$ | |
|---|---|---|---|---|---|---|---|---|
| R | 1.22 | 1.22 | 813 | 0.45 | | 74 | 0.027 | |
| Cr | 1.22 | 1.22 | 813 | MP<br>0.70 | mP<br>0.81 | 65 | MP<br>0.037 | mP<br>0.043 |
| Cl | 0.07 | 1.22 | 813 | OSL<br>0.45 | ISL<br>0.57 | 68 | OSL<br>0.025 | ISL<br>0.032 |

R = round, Cr = cross, Cl = clover

The exit profiles at $X = 0.5\ D_e$ of the streamwise velocity and the corresponding RMS from LDA measurements are shown in fig. 2 for the round jet fig. 2(a) and the lobed jets fig. 2(b) and (c), respectively. The mean streamwise velocity profiles of the circular jet in the vertical and the horizontal axis are flat and identical. That is not the case for the lobed jets when comparing velocity profiles along the major and the minor axis. In the major axis of the cross-shaped jet, the inflection point in the streamwise velocity profile is related to the inner shear layer at the junction of the central jet core and its lobes. As for the clover-shaped jet, due to closing of the center of the orifice, its principle characteristic is the quasi-absence of the central jet core. Hence, the flow is very weak in the minor axis. The two streams in the major axis, one on in each side of the central point, correspond to the flows in the aligned lobes.

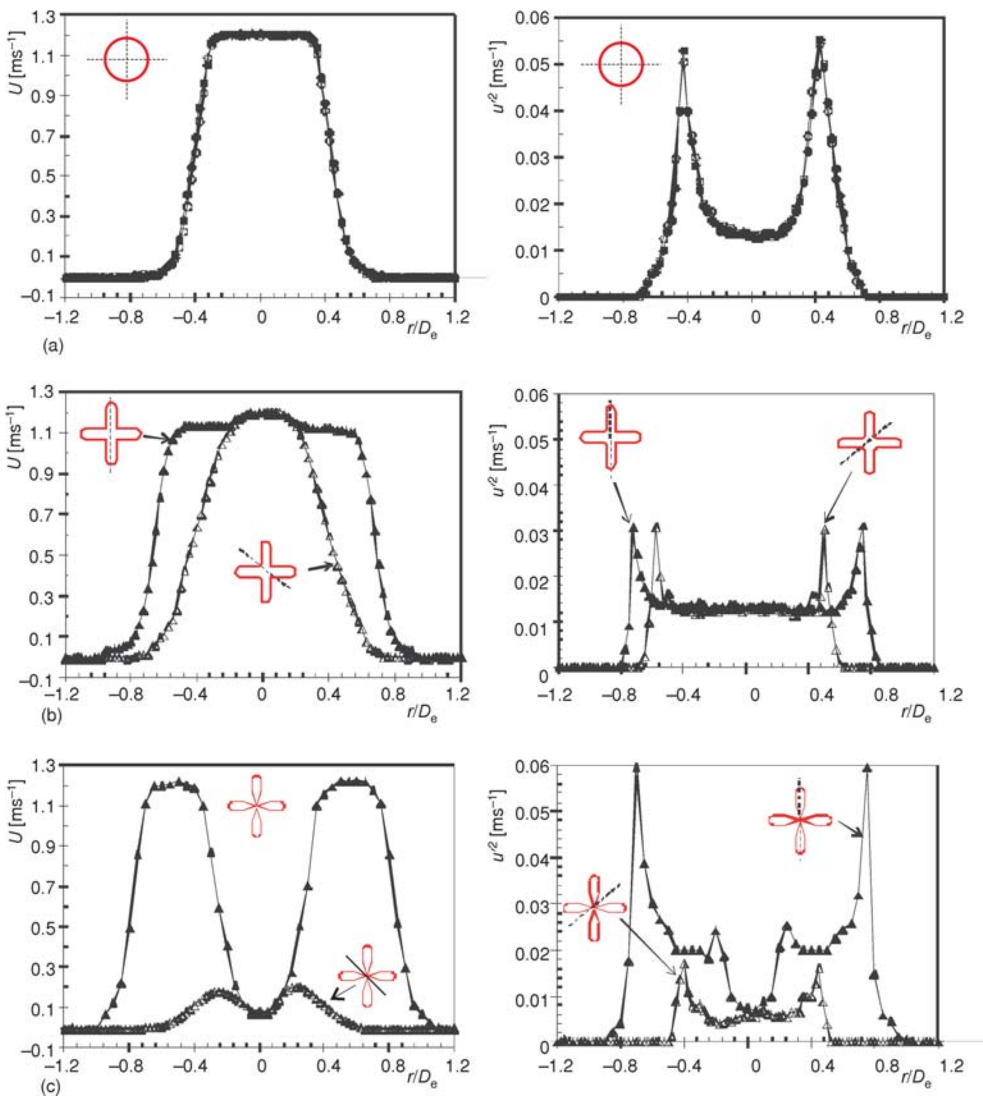

**Figure 2. Jet inlet profiles measured with LDA at $X = 0.5\ D_e$; streamwise mean velocity profiles (left) and the corresponding RMS profiles (right); (a) round jet, (b) cross-shaped jet, and (c) clover-shaped jet**

The turbulent profile is flat, at less than 2% of $U_{0max}$ in the central region for the circular jet and the cross-shaped jet. In the region of the shear layer, the turbulence increases in both jets. This increase is about 4% for the circular jet and 2% for the cross-shaped jet. As expected, the turbulent intensity is quite high in regions where the local shear in the mean streamwise velocity is large. The turbulence in the clover-shaped jet is also weak (less than 1% of $U_{0max}$ in the jet center) and increases to about 5% and 1.5% of $U_{0max}$ in the outer regions of major and minor axis, respectively. In the major axis of this jet, the presence of four peaks in the turbulence profile indicates the existence of a doubled shear layer: the outer shear layer (OSL) and the inner shear layer (ISL).

For each jet, the natural frequency $f_n$ (tab. 1), which is related to the most growing instability at the jet exit, is captured using a Dantec 55P11 hot wire probe placed in the jet exit shear layer. The corresponding Strouhal number is evaluated using the initial momentum thickness $\Theta_0$ of the boundary layer as characteristic length. The momentum thicknesses are calculated using the exit $U$-profiles of fig. 2.

The literature reports that the Strouhal number for free circular jets at a Reynolds number ranging from $10^4$ to $10^5$ varies in the range 0.013 to 0.023. In the present study the Reynolds number is very low 813, which probably explains the higher value of 0.027 obtained in the case of the round jet (tab. 1). In the cross-shaped jet, the momentum thickness is different in the major plane (MP) and the minor plane (mP), leading to different values of Strouhal number based on the same frequency (0.037 and 0.043, respectively). In the clover-shaped jet, since the flow is very weak in the mP, the momentum thickness is calculated only in the MP taking into account the presence of two shear layers. The Strouhal number is found lower in the OSL than in the ISL, *i. e.* 0.025 and 0.032, respectively.

## Results and discussion

### *Mean flow fields*

Figures 3 and 4 give the flow field views in the transversal cross-sections $0.5D_e \leq X \leq 5D_e$ of the cross-shaped jet, and the clover-shaped jet, respectively. Qualitative comparison of the two jets contours does not allow their classification in terms of their entrainment capability. In fact, at $X = 5D_e$, each jet has a specific geometry, cross-shaped (switched with 45° relative to the initial position) for the cross-jet and quasi-rectangular (with a deficit in streamwise velocity at the jet's center) for the clover-jet.

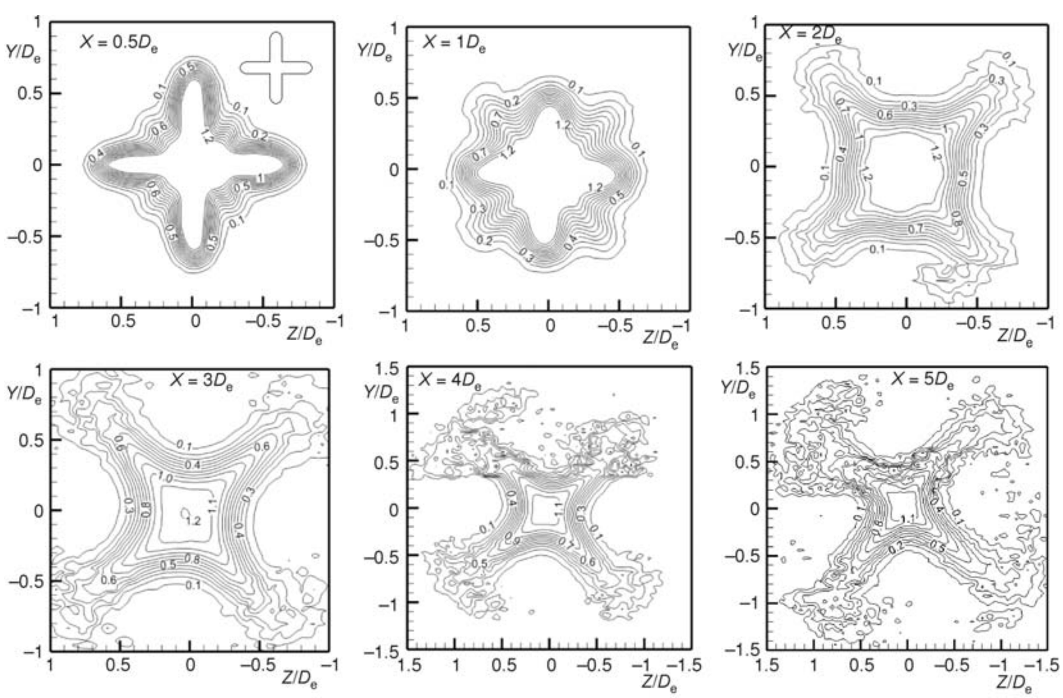


**Figure 3. Streamwise velocity contours $U$ [ms$^{-1}$] in transverse planes of cross-shaped jet**

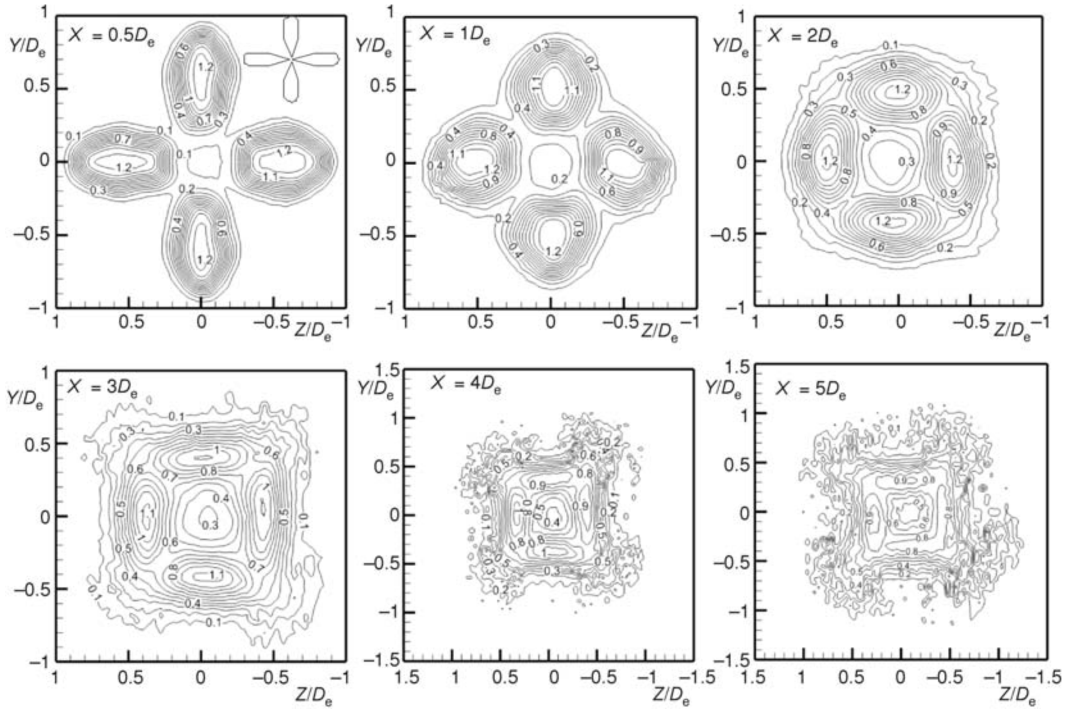

**Figure 4. Streamwise velocity contours U[ms$^{-1}$] in transverse planes of clover-shaped jet**

Initially, the clover jet (fig. 4) undertakes a global axis-switching as in the cross jet (fig. 3), but the phenomenon never complete in the former, whereas in the later, the switching-over is totally achieved at $X = 2D_e$. Indeed, the development of streamwise structures in the troughs of the clover orifice seems prevented, probably by the inner shear layer. However, one can observe a local switching-over, specific to flow deformation of each lobe. These local deformations have the effect of *filling* the flow deficits between the lobes.

The mechanisms at the origin of flow deformation of the cross-shaped and the clover-shaped jets are summarized in fig. 5. Based on mean vorticity component $\omega_x$ fig. 5 (1) and the $\lambda_2$ criterion fig. 5 (2) applied to the in-plane velocity field ($V$, $W$) at $X = 0.5\ D_e$, a set of streamwise structures are evidenced in each lobed jet and a schema of the underlying mechanism and its effect on each flow is proposed fig. 5 (3). In the cross-shaped jet fig. 5(1a), (2a), and (3a), on the peak of the lobe a pair of vortical structures is formed. The fluid between the two vortices of a pair is induced inward. This vortex pair is referred to as the *inflow pair*. The inflow vortices would result in a contraction of the jet cross-section in the MP. When considering the two vortices, one at each side of an orifice through, they form an *outflow pair*, as the fluid between these two vortices is expelled outside the jet. The outflow vortices would result in an expansion of the jet cross-section in the mP.

At $X = 3D_e$ figs. 6, (1a) and (2a), although the axial vorticity and $\lambda_2$ distributions are similar than the ones at $X = 0.5\ D_e$, their levels become lower due to the jet dilution by ambient air entrainment which is estimated farther (see section *Entrainment and jet throw*).

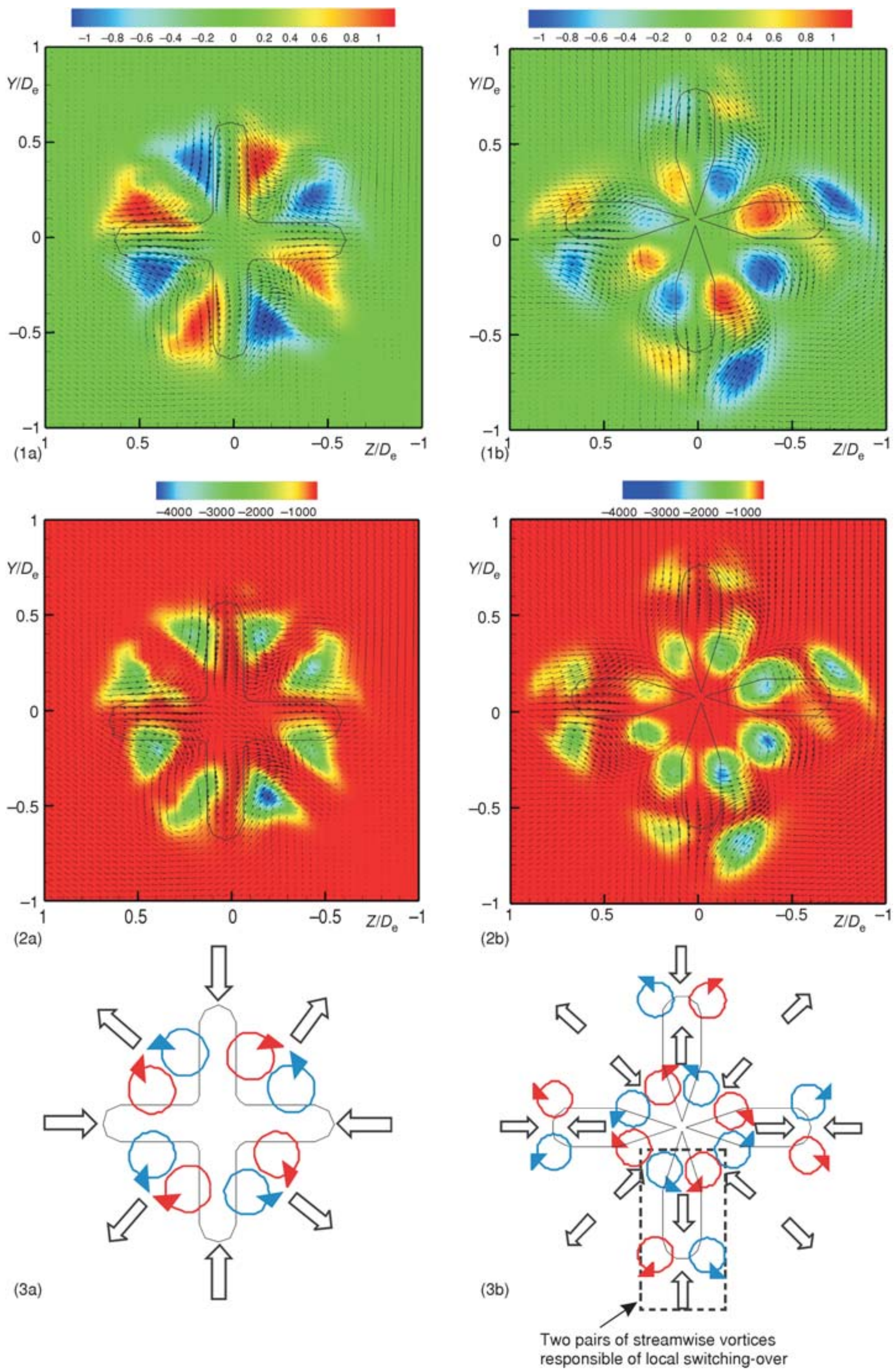


**Figure 5. (1) Mean streamwise vorticity $\omega_x$ at $X = 0.5D_e$ (2) $\lambda_2$ distributions at $X = 0.5D_e$ (3) Schematic of streamwise structures organization**

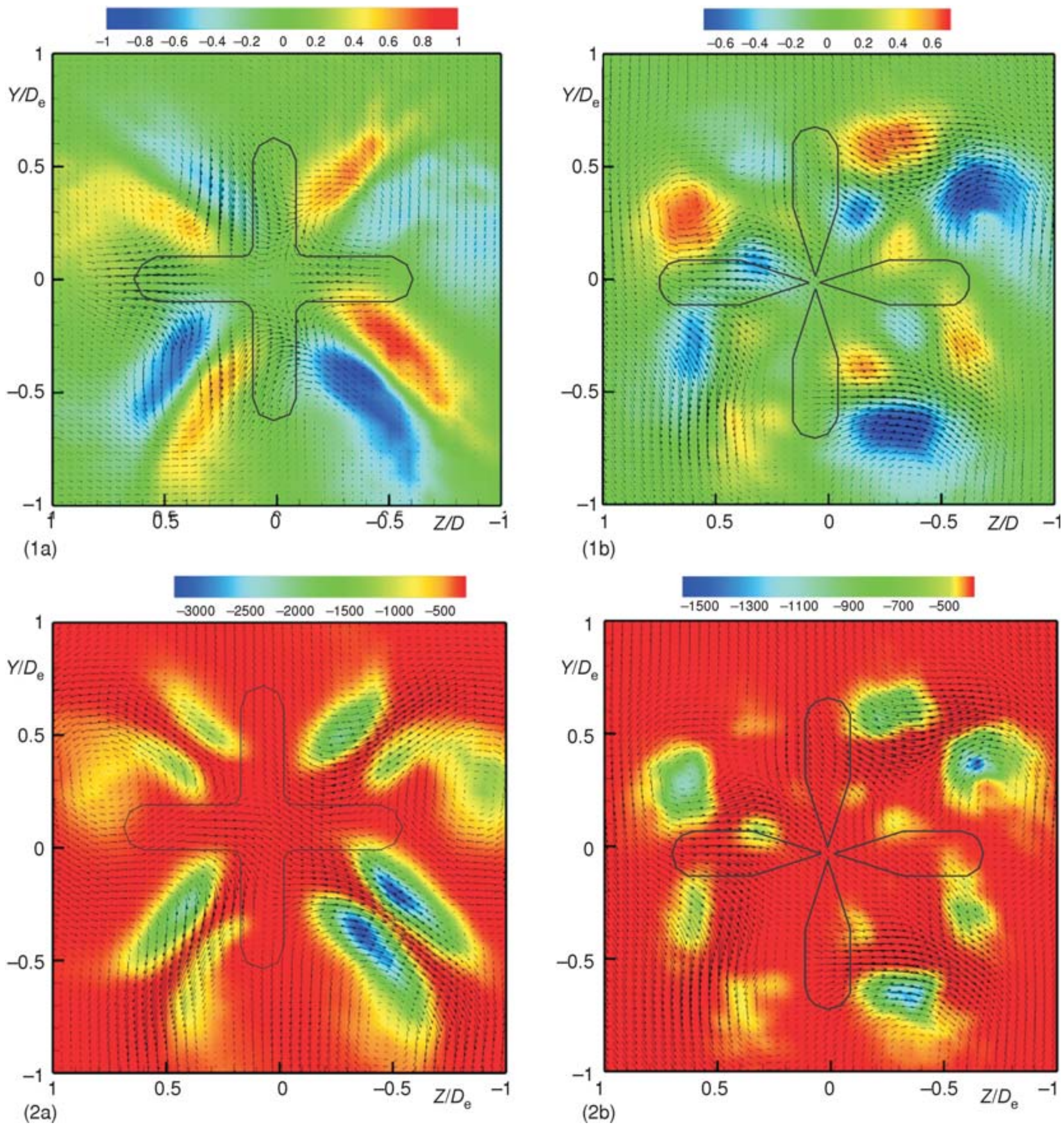


**Figure 6. (1) Mean streamwise vorticity $\omega_x$ at $X = 3D_e$ (2) The $\lambda_2$ distributions at $X = 3D_e$, – (a) cross-shaped jet, (b) clover-shaped jet**

In the clover-shaped jet figs. 5(b) and 6(b), streamwise structures are organized differently. Two crowns of counter-rotating pairs of streamwise structures are present. The outer crow is similar to the one of cross-shaped jet and is generated by the same mechanism. The additional internal crown of vortices which opposes the previous one is due to internal shear generated by closing the center of the orifice, see fig. 2 (c). Hence, it is expected that ambient air entrainment is lower in this jet in comparison to the case of cross-shaped jet. The local switching-over taking place at each lobe (fig. 4) can be explained by the effect of the two opposite streamwise pairs present at each lobe, evidenced in fig. 5 (3b) by a dashed rectangle.

### *Entrainment and jet throw*

Streamwise evolutions of the volumetric flow rate for both lobed jets and for the reference round jet are presented in fig. 7 (a), where $Q$ represents the volumetric flow rate calculated by $Q = \int U\mathrm{d}S$ with a fixed criteria of $U > 0.10$ m/s, and $Q_0$ the initial volumetric flow rate. In fig. 7(b) the entrained volumetric flow rate of the lobed jets are normalized with the one of the reference round jet. It appears that the flow entrained in the cross-shaped jet reaches almost 3.5 times the ambient flow entrained by the reference round jet and decreases to a ratio of 2 at 5 $D_e$.

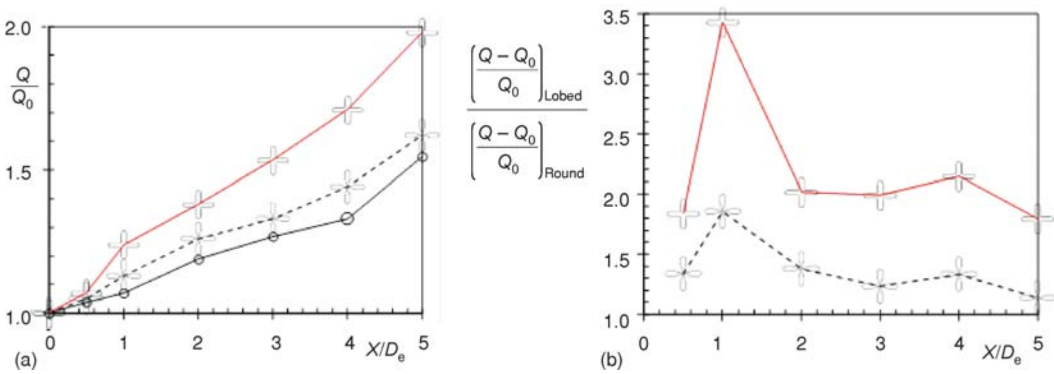


**Figure 7. (a) Streamwise evolution of the volumetric flow rates for the round jet and the lobed jets (cross and clover) at the same initial Reynolds number; (b) Streamwise evolution of the ratio between the entrained volumetric flow rates for the lobed jet and the reference round jet**

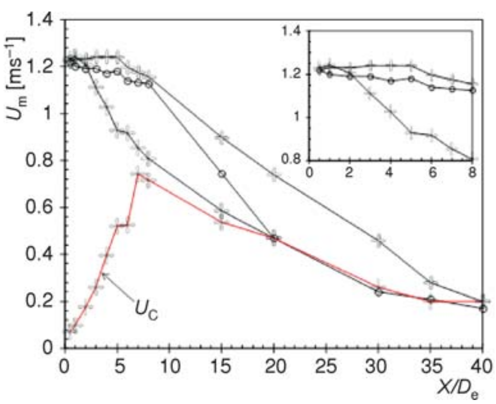


**Figure 8. Streamwise evolution of maximum velocity $U_m$ for the round jet, the cross-shaped jet and the clover-shaped jet. The subfigure gives a zoom on the near-field region.The $U_C$ is the centerline velocity in the clover-shaped jet**

As expected, for the clover-shaped jet, the entrained volumetric flow rate is lower than that in the cross-jet, due to the adverse effect of the counter-rotating inner crow of streamwise vortices evidenced earlier in figs. 5(b) and 6(b). The maximum induction gain relative to the round jet is 80% at $X = 1D_e$ and decrease rapidly to reach 20% at $5D_e$.

The changes in maximum velocity ($U_m$) of the three jets are compared in fig. 8. In the same figure, centerline velocity ($U_C$) of the clover-shaped jet is also reported. This jet has the peculiarity of having no potential core region. The coalescence effect of the four lobe flows tends to *fill* flow deficit at the jet center. Consequently, centerline velocity ($U_C$) of this jet increases continuously until $X = 7D_e$. After that position, $U_C$ decreases as $U_m$ of the same jet; the difference between $U_m$ and $U_C$ becomes negligible at $X = 1D_e$.

Although the decreasing rates of maximum velocity of the three jets are different, it is interesting to note that all the jets have the same velocity in the far region, at $X = 40D_e$. In the jet the near field, maximum velocity decreases faster in the clover-shaped jet, probably due to lobe flows interaction and to the subsequent reorganization of the four flows in single flow fig. 4.

## Conclusions

The present study analyses the influence of the geometry of the lobes in the orifice cross-shaped jet. Two cross-shaped orifices, one with open center and one with closed center are compared. The jet coming from a cross-shaped orifice with an open center has been shown in the past to provide substantial increase in the near field convective transport-mixing.

In the present study we are interested by the modification of local shears in the troughs of the cross-shaped jet, when orifice troughs are modified, such as the center of the orifice becomes closed, leading to a clover-shaped orifice. In the clover-shaped jet, a deformation of the global velocity field both in major and minor planes is the cumulative effect of two phenomena: (1) a local switching-over of the flow generated by one elementary clover lobe and (2) the coalescence of the parallel lobe flows which tends to *fill* the flow deficits at the jet center.

It is shown that streamwise structures are organized differently in the clover jet compared to the classical cross jet. Two crowns of counter-rotating pairs of streamwise structures are present in the clover jet. The outer crown is similar to the one of the cross jet and is generated by similar mechanism. The additional internal crown of vortices which opposes the previous one is due to internal shear generated by the closing of the center of the orifice. This explains the lower entrainment rates found in the clover-shaped jet compared to the cross-shaped jet.

## Acknowledgments

This work was supported by Grants of the French National Agency for Research, ANR, Indubat – Programme Prebat- Volet Technologique – 2005 – Contrat n° 0507C0084 and of the Romanian National Authority for Scientific Research, CNCS, UEFISCDI, Project number: PN-II-PT-PCCA-2011-3.2-1212

## References

[1] Suprayan, R., Fiedler, H. E., On Streamwise Vortical Structures in the Near-Field of Axisymmetric Shear Layers, *Meccanica, 29* (1994), 4, pp. 403-410
[2] Liepmann, D., Gharib, M., The Role of Streamwise Vorticty in the Near Field Entrainement of Round Jets, *Journal of Fluid Mechanics, 245* (1992), Dec., pp. 642-668
[3] Husain, Z. D., Hussain, A. K. M. F ., Natural Instability of Free Shear Layers, *AIAA Journal, 21* (1983), 11, pp. 1512-1517
[4] Brown, G. L., Roshko, A., On Density Effects and Large Structures in Turbulent Mixing Layers, *Journal of Fluid Mechanics, 64* (1974), 4, pp. 775-816
[5] Becker, H. A., Massaro, T. A., Vortex Evolution in a Round Jet, *Journal of Fluid Mechanics, 31* (1968), 3, pp. 435-448
[6] Crow, S. C., Champagne, F. H., Orderly Structure in Jet Turbulence, *Journal of Fluid Mechanics, 48* (1971), 3, pp. 547-591
[7] Toyoda, K., Hiramoto, R., Effect of Streamwise Vortices on Characteristics of Jets, *JSME International Journal Series B, 49* (2006), 4, pp. 884-889
[8] Todde, V., *et al.*, Experimental Analysis of Low-Reynolds Number Free Jets, Evolution along the Jet Centerline and Reynolds Number Effects, *Experiments in Fluids, 47* (2009), 2, pp. 279-294
[9] Mathew, J., Basu, A. J., Some Characteristcs of Entrainment at a Cylindrical Turbulence Boundary, *Physics of Fluids, 14* (2002), 7, pp. 2065-2072
[10] Liepmann, D., Streamwise Vorticity and Entrainment in the Near Field of a Round Jet, *Physics of Fluids, 3* (1991), 5, pp. 1179-1185
[11] Gutmark, E. J., Ho, C. M., Preferred Modes and the Spreading Rates of Jets, *Physics of Fluids, 26* (1983), 10, pp. 2932-2938
[12] Zaman, K. B. M. Q., Streamwise Vorticity Generation and Mixing Enhancement in Free Jets by Delta Tabs, AIAA Shear Flow Conference, Orlando, Fla., USA, 1993
[13] Gutmark, E. J., Grinstein, F. F., Flow Control with Noncircular Jets, *Annual Reviews of Fluid Mechanics, 31* (1999), Jan., pp. 239-272

[14] New, T. H., An Experimental Study on Jets Issuing from Elliptic Inclined Nozzles, *Experiments in Fluids, 46* (2009), 6, pp. 1139-1157
[15] Husain, H. S., Hussain, A. K. M. F., The Elliptic Whistler Jet, *Journal of Fluid Mechanics, 397* (1999), Oct., pp. 23-44
[16] Nastase, I., Meslem, A., Vortex Dynamics and Mass Entrainment in Turbulent Lobed Jets with and without Lobe Deflection Angles, *Experiments in Fluids, 48* (2010), 4, pp. 693-714
[17] Hussain, F., Husain, H. S., Elliptic Jets, Part1. Characteristics of Unexcited and Excited Jets, *Journal of Fluid Mechanics, 208* (1989), Nov., pp. 257-320
[18] Hu, H., *et al*., A Study on a Lobed Jet Mixing Flow by Using Stereoscopic Particle Image Velocimetry Technique, *Physics of Fluids, 13* (2001), 11, pp. 3425-3441
[19] El-Hassan, M., *et al*., Experimental Investigation of the Flow in the Near-Field of a Cross-Shaped Orifice Jet, *Phys. Fluids, 23* (2011), 4, 045101
[20] El-Hassan, M., Meslem, A., Time-Resolved Stereoscopic PIV Investigation of the Entrainment in the Near-Field of Circular and Daisy-Shaped Orifice Jets, *Physics of Fluids, 22* (2010), 3, 035107
[21] Nastase, I., *et al*., Primary and Secondary Vortical Structures Contribution in the Entrainment of Low Reynolds Number Jet Flows. *Experiments in Fluids, 44* (2008), 6, pp. 1027-1033
[22] Meslem, A., *et al.*, Analysis of Jet Entrainment Mechanism in the Transitional Regime by Time-Resolved PIV, *Journal of Visualization, 14* (2011), 1, pp. 41-52
[23] Wang, X. K., *et al*., On the Near-Field of a Square Jet with Vortex-Generating Tabs, *Fluid Dynamics Research, 32* (2003), 3, pp. 99-117
[24] Mishra, D. P., Kumar, P., Experimental Study of Bluff-Body Stabilized LPG-H2 Jet Diffusion Flame with Preheated Reactant, *Fuel, 89* (2010), 1, pp. 212-218
[25] Jeong, J., Hussain, F., On the Identification of a Vortex, *Journal of Fluid Mechanics, 285* (1995), Feb., pp. 69-94
[26] Dubief, Y., Delcayre, F., On Coherent-Vortex Identification in Turbulence, *Journal of Turbulence, 1* (2000), 11, pp. 1-22

Paper submitted: July 24, 2013
Paper revised: November 28, 2013
Paper accepted: December 2, 2013